Laser Excited Emission Spectroscopy of Azulene in the Gas Phase

DAN HUPPERT AND JOSHUA JORTNER
Department of Chemistry, Tel-Aviv University, Tel-Aviv, Israel
AND
PETER M. RENTZEPIS
Bell Telephone Laboratories, Incorporated, Murray Hill, New Jersey 07974

(Received 19 January 1972)

In this paper we present the results of an experimental study of the radiative decay of the two lowest singlet states S_1 and S_2 of the azulene molecule in the gas phase excited by a Q switched ruby laser (14 400 cm^{-1}) and by its second harmonic (28 800 cm^{-1}). Spectroscopic information has been obtained concerning the energy resolved spectra of the $S_1 \rightarrow S_0$ and of the $S_2 \rightarrow S_1$ emission. The quantum yield data for the $S_1 \rightarrow S_0$ decay led to an estimate of the nonradiative decay time of S_1. The branching ratio between the $S_2 \rightarrow S_0$ and the $S_2 \rightarrow S_1$ emissions was utilized for the evaluation of the $S_2 \rightarrow S_1$ radiative decay time. The study of the consecutive two photon $S_0 \rightarrow S_1 \rightarrow S_2$ excitation leads to an estimate of the $S_1 \rightarrow S_2$ absorption cross section near the electronic origins of the two excited states. The decay characteristics of the lowest excited singlet state of the "isolated" azulene molecule confirm the theoretical prediction concerning nonradiative electronic relaxation in the statistical limit.

I. INTRODUCTION

Efficient nonradiative decay processes[1] were blamed for the lack of observable emission from highly excited electronic states of most large molecules, and from the first excited state of a few abnormal molecules, such as azulene[2–5] and its derivatives.[6,7,8] The recent utilization of mode locked high power solid state lasers as optical excitation sources,[9,10,11] compensates for these low emission yields. Extremely low fluorescence quantum yields $\sim 10^{-6}$, resulting from the radiative decay (to the ground state) of the first metastable excited singlet state of azulene[12,13] and of benzophenone[14] in solution were observed. Similar techniques were applied for the observation of the time and energy resolved resonance fluorescence from the second excited singlet state of some large molecules in the low pressure gas phase[15] (3,4-benzpyrene and napthalene). Finally this method was applied[16] for the detection of weak fluorescence originating from the transition between the second and first excited singlet states of azulene in solution. These new spectroscopic techniques[10–16] provide direct information concerning the spectral distribution of the weak fluorescence, and indirect information concerning electronic relaxation processes obtained from the emission quantum yields. Direct interrogation[11–14] of electronic and vibrational relaxation in excited states of large molecules was accomplished by the development of the techniques of picosecond spectroscopy.[11]

In this paper we report the results of a spectroscopic study of the radiative decay of the two lowest excited singlet states (S_1 and S_2) of the azulene molecule in the gas phase excited by a Q switched Ruby laser. The decay characteristics of this molecule, previously studied in solution[11,12] by the direct methods of picosecond spectroscopy,[13] provide the best known example for the violation of Kasha's rules.[17] The laser pulse width employed in the present work considerably exceeds the decay times of both S_1 and S_2 states, so we are concerned here with steady state emission spectroscopy, resulting from "brute force" excitation by high energy source. The motivations for this study are:

(a) The theory of electronic relaxation processes predicts that in the statistical limit[1] an inert medium (which does not modify the zero order molecular levels or the interstate coupling) will not affect the gross nonradiative decay characteristics. There are very few experimental data available to support this conclusion. For example, it is known that the decay time and fluorescence quantum yield of the first excited singlet state of anthracene, are practically identical in the gas phase and in solution.[18,19] Similar observations were reported for the lowest excited singlet state of biacetyl,[20] however recent gas phase quenching data[21] seem to be in variance with this observation. The major relaxation pathway of the azulene S_1 state involves internal conversion to the ground state.[12] This physical situation definitely corresponds to the statistical limit[1] as for the (relatively low) S_0–S_1 electronic gap $\Delta E \sim 14\,200$ cm^{-1} the total density of states in the S_0 manifold, which are quasidegenerate with S_1, is $\rho_l \sim 10^{11}$ cm. The upper limit for the recurrence time[1] is $\hbar\rho_l \sim 0.5$ sec, which exceeds by ten orders of magnitude the experimental values for nonradiative decay times of S_1 in solution.[11,12] $\tau_{nr} = 7.5\times10^{-12}$ sec (for ν_5; S_1); $\tau_{nr} = 6\times10^{-12}$ sec (for ν_0; S_1) and $\tau_{nr} = 8\times10^{-12}$ sec (for the repopulation of the ground state). The azulene S_1 state definitely confirms to the theoretical criteria for the statistical limit, and it will be interesting to obtain complementary data, pertaining to electronic relaxation in the gas phase.

(b) The techniques of picosecond spectroscopy[9–16] utilize ultrashort (10^{-12} sec) high power (1–10 GW) pulses. It is interesting to inquire whether the same indirect information pertaining to the electronic relaxation characteristics of the metastable S_1 state will result from high energy, moderately low power (0.1 GW) "long time" (10 nsec) excitation.

(c) The spectroscopic data previously obtained for the $S_1 \rightarrow S_0$ and $S_2 \rightarrow S_1$ emission spectra of azulene in solution were measured[16] utilizing high power pulses. It is interesting to inquire whether the same results regarding the spectral distribution and the quantum yields will result from higher energy lower power excitation. In particular, under picosecond excitation to S_2 in solution stimulated $S_2 \rightarrow S_0$ emission may result, diminishing the effective quantum yield of the $S_2 \rightarrow S_1$ emission.

(d) The $S_2 \rightarrow S_1$ emission spectrum of azulene in solution previously recorded[16] in the spectral range 7000–8000 Å did not exhibit a vibrational structure. As radiative transitions between electronically excited states are interesting, it is worthwhile to study the $S_2 \rightarrow S_1$ emission over a wider spectral region.

II. EXPERIMENTAL METHODS

A. Optical Cell

Azulene samples were placed into the lower part of the cell consisting of a 30 cm long Pyrex tube connected at its upper end to a 2×1 cm optical fused quartz cell. The cell was placed in an oven constructed from a 40 cm long (5 cm diameter, thickness 1.5 mm) metal tube, surrounded by heating elements. Three quartz windows were sealed to the upper part of this tube, at the height of the optical cell, so that emission was monitored perpendicular to the exciting laser beam. The lower and the upper parts of the oven were heated separately utilizing conventional temperature control units (temperature stability ±1°C). For measurements in the 100–200°C temperature range a 10–20°C temperature differential was maintained between the upper and the lower parts of the cell. This procedure insured that no azulene condensed on the windows of the optical cell.

B. Gaseous Samples

The azulene samples (Fluka Puris grade) were further purified by sublimation, although this procedure proved later on to be unnecessary. The vapor pressure of liquid azulene (melting point 99°C) was previously recorded. From the gas phase absorption spectra (Fig. 1) and from the absorption coefficients for the $S_0 \rightarrow S_1$ transition in solution,[22] we can roughly estimate the vapor pressure to be ~15 torr at 135°C (while direct vapor pressure measurements yielded ~25 torr at this temperature) and ~100 torr at 195°C. Preliminary attempts to observe near infrared emission from gaseous azulene excited by a Q switched ruby laser (6943 Å) resulted in disastrous results, as after exposing the sample to a few laser pulses, a buildup of a parasitic emission in the visible and near infrared region was observed and which was characterized by a decay time of ~100 nsec. Simultaneously the cell windows were covered with a greenish deposit. These undesirable effects may arise from the

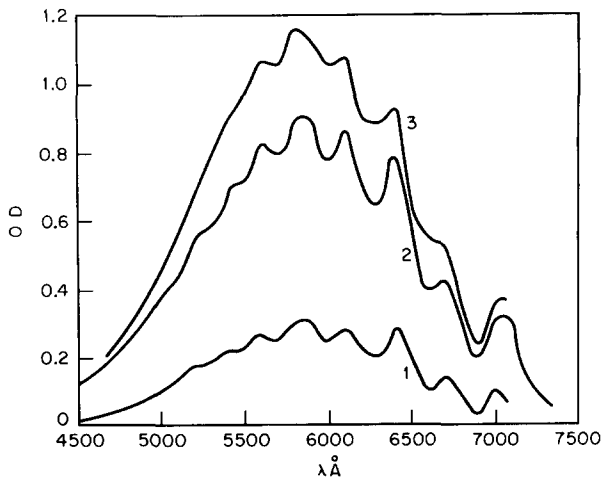

FIG. 1. $S_0 \rightarrow S_1$ absorption spectra of gaseous azulene. (1) 100°C (2) 135°C (3) 195°C.

efficient $S_1 \rightarrow S_0$ internal conversion resulting in a ground state molecule with ~14 000 cm^{-1} excess vibrational energy, that prior to vibrational relaxation by collisions, yields a new (unidentified) chemical product by a unimolecular reaction or by interacting with another "vibrationally cold" ground state molecule. Introduction of an inert buffer helium gas at 250 torr at 30°C completely eliminates this spurious fluorescence. All our experiments were performed on gaseous azulene containing 0.015M He, which was introduced after evacuation of the cell up to 10^{-5} torr. The experimental data were reproducible upon thermal cycling of the cell. Our experiments were performed in the temperature range 130–200°C. $S_0 \rightarrow S_1$ and $S_0 \rightarrow S_1 \rightarrow S_2$, excitations were carried out at 195°C (0.22 OD at 6943 Å) while the $S_0 \rightarrow S_2$ excitation was performed at 135°C (0.3 OD at 3472 Å).

C. Laser Sources

Excitation of azulene into the vicinity of the vibrationless level of S_1 (see Fig. 1) and consecutive $S_0 \rightarrow S_1 \rightarrow S_2$ excitation into S_2 was performed by 6943 Å light from a Q switched (by cryptocyanine and vanadyl phthalocyanine dyes) ruby laser. A 4 in.×9/16 in. rod delivered 50 MW/cm² with a pulse half-width of 20 nsec, while a 6.5 in.×5/8 in. rod delivered 200 MW/cm² with a pulse half-width of 10 nsec. Direct $S_0 \rightarrow S_2$ excitation was provided by a 3472 Å pulse from the second harmonic of the ruby laser generated by a KDP crystal, which was characterized by a power of 0.5–1.0 MW/cm² (after filtration of the first harmonic by $CuSO_4$ solution). The intensity of each exciting pulse was determined in each experiment by reflecting a small portion of the beam to photodiodes.

D. Emission Spectra

Energy resolved luminescence spectra resulting from the $S_1 \rightarrow S_0$ transition (6943 Å excitation) and from the

$S_2 \rightarrow S_1$ transition (3472 Å excitation), both observed in the spectral region 7200–9300 Å were monitored by a 250 mm Jarrel–Ash monochromator at a resolution of 25 Å. In view of the broad structureless emission bands observed, this low resolution was sufficient. These emissions were measured by RCA 7102 (S1) and Phillips TVP 56 (S20) photomultipliers. For the measurements of the $S_2 \rightarrow S_0$ emission in the spectral region 3600–4500 Å resulting from direct $S_0 \rightarrow S_2$ excitation (at 3472 Å) and from consecutive $S_0 \rightarrow S_1 \rightarrow S_2$ excitation (at 6943 Å) we have used a Phillips TVP 56 (S20) photomultiplier. Appropriate glass and solution filters were placed in front of the detectors to remove scattered light. The spectral resonance of the whole detection system (monochromator and photomultiplier) was calibrated by a tungsten lamp.

E. Estimates of Quantum Yields

The quantum yield for the $S_2 \rightarrow S_1$ emission was determined by the measurement of the branching ratio between the $S_2 \rightarrow S_1$ and the $S_2 \rightarrow S_0$ emissions resulting from 3472 Å excitations using the same setup employed for the spectroscopic emission studies. The $S_2 \rightarrow S_1$ emission was determined at $\lambda_2 = 7300$, 7400, and 7500 Å while the $S_2 \rightarrow S_0$ emission was measured at $\lambda_1 = 4300$, 4400, and 4500 Å. The intense blue fluorescence was attenuated by calibrated neutral density filters. From the knowledge of the distributions of the two emissions and the relative emission yields at several selected wavelengths λ_1 and λ_2 we could determine the ratio R of the total blue to the total infrared emission. From our solution data[23] we have found that this ratio is the same within a numerical factor of 2 in the gas phase and in solution. The $S_2 \rightarrow S_0$ emission quantum yield in the gas phase is unknown. We have compared the $S_2 \rightarrow S_0$ emission quantum yields of azulene in the gas phase and in solution, excited in the spectral region 3500–3100 Å, utilizing a Perkin Elmer Hitachi spectrofluorimeter. The quantum yields in the gas phase and in solution are the same within an uncertainty of 50%. We thus use the quantum yield $Y = 0.2$ determined by Berlman[24] for the $S_2 \rightarrow S_0$ emission in solution for the determination of the $S_2 \rightarrow S_1$ emission quantum yield in the gas phase.

The quantum yield for the $S_1 \rightarrow S_0$ emission can be directly determined provided that the absolute efficiency of the monitoring system (monochromator and photomultiplier) is known. We have chosen an alternative method, based on the determination of the relative $S_1 \rightarrow S_0$ emission intensity resulting from one (6943 Å) photon absorption and the $S_2 \rightarrow S_0$ emission intensity resulting from consecutive two (6943 A) photon absorptions at a few selected wavelengths followed by an absolute determination of the total blue fluorescence intensity. This approach is based on two stages: (a) The ratio of the $S_2 \rightarrow S_0$ and the $S_1 \rightarrow S_0$ emissions, both resulting from excitation by the first harmonic of the ruby laser was monitored, both measurements performed at the same laser intensity. This experiment utilized the same setup as employed for the determination of the quantum yield for $S_2 \rightarrow S_1$ emission. (b) The total yield of the $S_2 \rightarrow S_0$ emission resulting from consecutive two photon absorption by the first harmonic of the ruby laser was determined by removing the monochromator and monitoring the emission passed through appropriate filters in the range 3600–4500 Å by an RCA IP 39 (S4) photodiode. Utilizing these results with the absolute intensity of the laser pulse and the OD of the vapor, we could then determine the absolute quantum yield for the $S_1 \rightarrow S_0$ emission. Note that this procedure does not require the absolute value of the $S_2 \rightarrow S_0$ emission yield. An alternative method, based on the comparison of the emission quantum yields for the $S_2 \rightarrow S_0$ emission excited at 3472 Å and the $S_1 \rightarrow S_0$ emission excited at 6943 Å and setting as before $Y(S_2 \rightarrow S_0) \approx 0.2$ led to the same result within 50%, as obtained from the first method.

F. Cross Section for $S_1 \rightarrow S_2$ Absorption

The total intensity of $S_2 \rightarrow S_0$ fluorescence resulting from consecutive two photon absorption $S_0 \rightarrow S_1 \rightarrow S_2$ excited by 6943 Å ruby light was monitored in the range 3600–4500 Å by a RCA IP 39 (S4) photodiode, screened by appropriate filters. From the dependence of the emission intensity on the laser intensity, from the $S_0 \rightarrow S_1$ cross section and the quantum yields for $S_1 \rightarrow S_0$ and $S_2 \rightarrow S_0$ emission, we were able to estimate the cross section for the $S_1 \rightarrow S_2$ absorption at 6943 Å.

G. Data Processing

The photomultiplier output (amplified when necessary by HP amplifiers) was displayed on a Tetronix 454 oscilloscope and photographed. The decay times of the $S_2 \rightarrow S_0$, $S_2 \rightarrow S_1$ and $S_1 \rightarrow S_0$ emissions were short relative to the pulse length (10–20 nsec). Numerical integration of the oscilloscope traces were performed to obtain the emission intensity. The number of photographs used for each point was 4–6. The final values for the energy dependent emission spectra are accurate within $\pm 10\%$. It is more difficult to assess the accuracy of our experimental data for the quantum yields and for the cross section for $S_1 \rightarrow S_2$ absorption. We believe that our experimental value for the quantum yield for $S_1 \rightarrow S_0$ emission is accurate within a numerical factor of 2, while the quantum yield for the $S_2 \rightarrow S_1$ emission and for the $S_1 \rightarrow S_2$ absorption are accurate within a numerical factor of 4. The smaller accuracy of the latter data is due to the use of the value for the $S_2 \rightarrow S_0$ emission yield, which is known only within an uncertainty of a numerical factor of 2.

H. Background Determinations

Samples at room temperature were used for background determination. The amount of scattered light

in the $S_1 \rightarrow S_0$ emission (6943 Å excitation) was quite serious, but it did not exceed 15% of the signal, and was flat throughout the whole spectral region. The scattered light in the $S_2 \rightarrow S_1$ emission (induced by 3472 Å) and in the $S_2 \rightarrow S_0$ emission (resulting from consecutive $S_0 \rightarrow S_1 \rightarrow S_2$ excitation (6943 Å) did not exceed 1%.

III. RESULTS

A. Emission Spectroscopy

The intensity of the emission observed in the spectral region 7300–9300 Å resulting from 6943 Å excitation was linear with the exciting laser intensity (Fig. 2). These data imply that the process is linear and that saturation of absorption does not occur. The energy resolved spectrum, assigned to the $S_1 \rightarrow S_0$ transition (originating from the vicinity of the vibrationless level of S_1) is displayed in Fig. 3. This emission is broad and practically structureless. Only a weak modulation of the emission spectrum measured at 195°C is exhibited, forbidding any vibrational analysis. These results are somewhat disappointing, however they can be readily understood in terms of "trivial" temperature dependent broadening of absorption and emission lines of large molecules by sequence congestion.[25] It should be noted

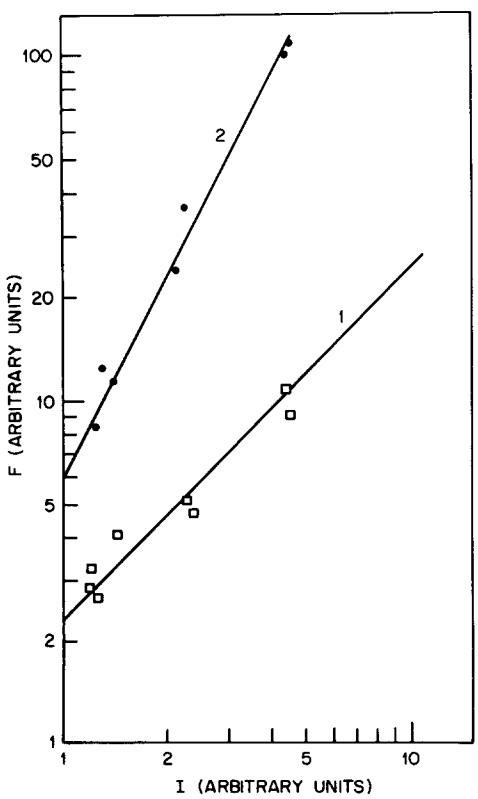

FIG. 2. The dependence of the $S_1 \rightarrow S_0$ and the $S_2 \rightarrow S_0$ fluorescence intensity on the intensity I of the exciting ruby laser (6943 Å). Curve 1: Fluorescence at 7600 Å, slope 1.0. Curve 2: Fluorescence at 3800 Å, slope 2.0.

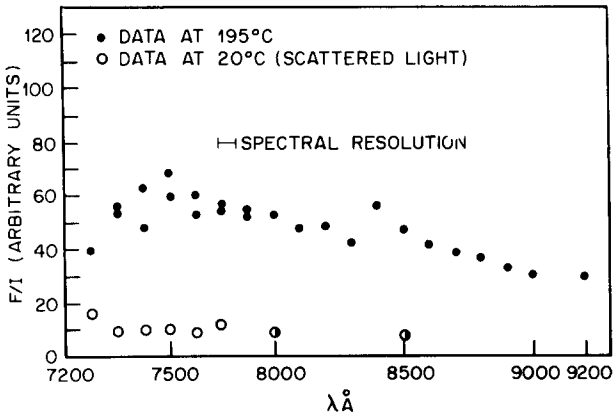

FIG. 3. The spectral distribution of the $S_1 \rightarrow S_0$ emission of gaseous azulene excited at 6943 Å (fluorescence normalized to laser intensity).

that at 195°C the $S_0 \rightarrow S_1$ absorption spectrum (see Fig. 1) is also almost completely diffuse. The smearing out of the $S_0 \rightarrow S_1$ absorption (and $S_1 \rightarrow S_0$ emission) occurs in the same temperature region (150–200°C) as reported by Byrne and Ross[25] for the $S_0 \rightarrow S_2$ absorption. It was pointed out[25] that for a perfectly symmetrical band group the intensity maximum should not shift with temperature. The $S_0 \rightarrow S_1$ transition of azulene exhibits just the totally symmetric (900 cm^{-1}) vibration and indeed this prediction is confirmed (see Fig. 1). The maximum of the intensity distribution from the vibrationless S_1 level should be unaffected by the temperature. The maximum of the $S_1 \rightarrow S_0$ emission from gaseous azulene at 195°C (7600 Å) is in good agreement with the emission maximum at 7500 Å previously observed in solution at room temperature.[13]

The emission observed in the spectral region 7300–9300 Å resulting from $S_0 \rightarrow S_2$ excitation at 3472 Å near the electronic origin of S_2 is assigned to the $S_2 \rightarrow S_1$ fluorescence. This assignment rests on the location of that emission spectrum and on the reasonable correspondence between the long pure radiative decay time for the $S_2 \rightarrow S_1$ emission (see III.B) and the low cross section for the $S_1 \rightarrow S_2$ absorption (see III.C). This emission spectrum (Fig. 4) obtained at 135°C exhibits from quite pronounced broad bands peaking at 7350, 7900, 8500, and 9150 Å which are tentatively assigned to the vibronic components of the $S_2 \rightarrow S_1$ transition. The mean spacing between these bands is 850 ± 100 cm^{-1} which corresponds to the carbon stretching mode similar to that observed in the $S_0 \rightarrow S_1$ absorption (see Fig. 1). This gas phase emission spectrum is in qualitative agreement with the previously reported $S_2 \rightarrow S_1$ emission of azulene in methanol[16] in the region 7400–8000 Å and in good agreement with the $S_2 \rightarrow S_1$ emission of azulene and azulene-d_8 in methanol recently monitored[23] in the range 7400–9300 Å which exhibits a shoulder at 7600 Å followed by bands at 8000 Å, 8700 Å and 9300 Å. The lowest band in the gas phase (7350 Å) should be probably assigned either to the electronic

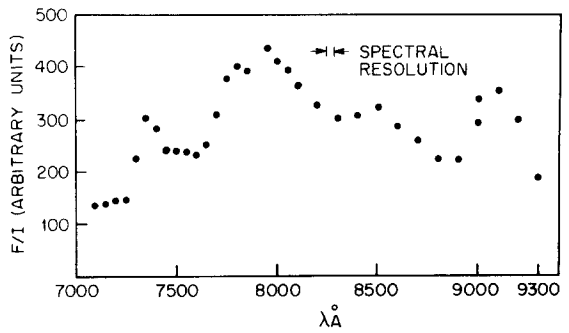

FIG. 4. The spectral distribution of the $S_2 \rightarrow S_1$ emission of gaseous azulene excited at 3472 Å (fluorescence normalized to laser intensity).

origin of the transition or more probably to the false origin of a vibronically induced transition.

B. Quantum Yields

The quantum yield Y $(S_1 \rightarrow S_0)$ for the $S_1 \rightarrow S_0$ emission [which is linear (see Fig. 2) in the exciting laser intensity] was determined by exciting the gaseous sample (OD = 0.22 at 6943 Å) by $I = 50$ MW for 20 nsec at 6943 Å, and by monitoring the $S_1 \rightarrow S_0$ and the $S_2 \rightarrow S_0$ (see III.B) emission resulting from this excitation. The ratio of the total emission yields in the regions 3600–4600 Å (blue) and 7300–9300 Å (infrared) was found to be $R_1 = 0.045$ at this laser power level while the total blue fluorescence was 8.1 W. Hence we get $Y(S_1 \rightarrow S_0) = 8 \times 10^{-6}$. Making use of the pure radiative lifetime, determined from the integrated oscillator strength[26] $\tau_r(S_1 \rightarrow S_0) = 8 \times 10^{-7}$ sec we can evaluate the nonradiative decay time $\tau_{nr}(S_1)$ for the electronic relaxation of the first excited singlet state. From the relation $Y(S_1 \rightarrow S_0) = \tau_{nr}(S_1)/[\tau_r(S_1 \rightarrow S_0) + \tau_{nr}(S_1)]$ we get $\tau_{nr}(S_1) = 7 \times 10^{-12}$ sec. The results for the emission quantum yield and for the nonradiative decay time for the decay in the vicinity of the S_1 origin are in good agreement with the solution data obtained by picosecond spectroscopy.[11,12]

The branching ratio $R = 450$ was determined for the total intensities of the $S_2 \rightarrow S_0$ and of the $S_2 \rightarrow S_1$ emissions resulting from 3472 Å excitation. The quantum yield $Y(S_2 \rightarrow S_1)$ for the $S_2 \rightarrow S_1$ emission is given by $Y(S_2 \rightarrow S_1) = Y(S_2 \rightarrow S_0)/R$, where we have taken the solution value[2] $Y(S_2 \rightarrow S_0) = 0.2$ (see II.E). Thus we obtain $Y(S_2 \rightarrow S_1) = 5 \times 10^{-4}$. For this result and from the pure radiative decay time[26] $\tau_r(S_2 \rightarrow S_0) = 5 \times 10^{-9}$ sec estimated from the integrated oscillator strength for $S_0 \rightarrow S_2$, we can estimate the pure radiative decay time $\tau_r(S_2 \rightarrow S_1)$. From $R = \tau_r(S_2 \rightarrow S_1)/\tau_r(S_2 \rightarrow S_0)$ we get $\tau_r(S_2 \rightarrow S_1) = 2 \times 10^{-6}$ sec. These gas phase data are also in good agreement with our recent solution data[23] where we have obtained $Y(S_2 \rightarrow S_1) = 2 \times 10^{-4}$ for the excitation of azulene in methanol solution by the second harmonic of a Q switched ruby laser. These data do not agree well with the original observation[16] of $Y(S_2 \rightarrow S_1) < 10^{-6}$ for azulene in methanol excited by the second harmonic of a mode locked ruby laser. A possible explanation for the discrepancy between these results is that excitation of azulene solution by the second harmonic of the mode locked ruby laser may generate stimulated $S_2 \rightarrow S_1$ emission, thus reducing the yield of the $S_2 \rightarrow S_1$ fluorescence. Low power excitation by a Q switched laser can safely rule out this possibility.

C. Consecutive Two Photon Absorption to S_2

As we have already stated in Sec. (III.C) 6943 Å excitation of gaseous azulene results in emission in the 3600–4500 Å region. These results concur with previous solution data.[12] The blue emission is attributed to the $S_2 \rightarrow S_0$ fluorescence resulting from consecutive $S_0 \rightarrow S_1$ followed by $S_1 \rightarrow S_2$ absorption. This interpretation rests on two experimental observations. First, the dependence of the intensity of the blue fluorescence on the square of the laser intensity I (see Fig. 2). From the measurement of the total blue fluorescence intensity, $F_B{}' = 1.6 \times 10^{20}$ photons $cm^{-3} \cdot sec^{-1}$ for $I = 1.8 \times 10^{24}$ photons $cm^{-2} \cdot sec^{-1}$, we get $F_B{}' = KI^2$ where $K = 5 \times 10^{-33}$ $photon^{-1}$ $cm \cdot sec^{-1}$. Second, the spectral distribution of this blue emission (see Fig. 5) is similar to the well-known $S_2 \rightarrow S_0$ azulene fluorescence in solution. We should note in passing that the consecutive $S_0 \rightarrow S_1 \rightarrow S_2$

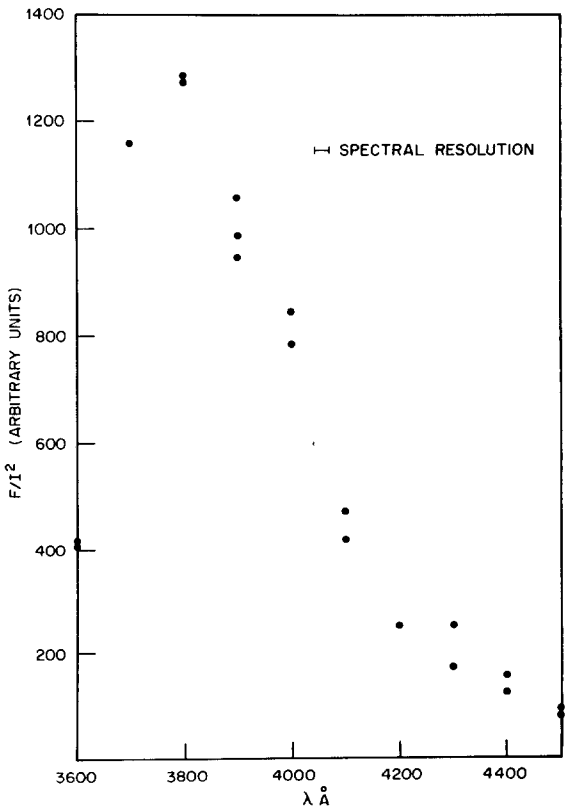

FIG. 5. The spectral distribution of the $S_2 \rightarrow S_0$ emission resulting from consecutive two photon excitation at 6943 Å (fluorescence normalized to the square of the laser intensity).

excitation by 6943 Å will result also in $S_2 \rightarrow S_1$ emission, which overlaps the $S_1 \rightarrow S_0$ fluorescence. However, at the laser power level ($I = 50$ MW) employed to monitor the spectral distribution and the quantum yield for the $S_1 \rightarrow S_0$ emission the (intensity dependent) ratio of the $S_2 \rightarrow S_0$ and the $S_1 \rightarrow S_0$ emission was found to be 4.5×10^{-2} while the branching ratio between the $S_2 \rightarrow S_0$ and the $S_2 \rightarrow S_1$ emissions is $R = 450$ (see III.B). Thus the ratio between the $S_2 \rightarrow S_1$ and the $S_1 \rightarrow S_0$ emissions resulting from 6943 Å excitation is only 10^{-4} and the contribution of the former emission can be safely neglected.

Turning now to a simple kinetic analysis of the consecutive excitation data (which is valid for radiative and nonradiative decay processes in the statistical limit) we consider the energy levels diagram presented in Fig. 6. Let $\sigma(S_i^{(0)} \rightarrow S_j^{(0)})$ be the absorption cross section between the electronic states i and j at 6943 Å (i.e., near the electronic origin of the first singlet for $S_0 \rightarrow S_1$ and near the electronic origin for the second singlet state for $S_1 \rightarrow S_2$). $\tau_r(S_i \rightarrow S_j)$ are the pure radiative lifetimes, the values of $\tau_r(S_j \rightarrow S_0)$ in the gas phase being estimated from the integrated oscillator strengths in solution (we thus neglect inner field corrections[22] which are probably of the order of 30%). $\tau_{nr}(S_j^{(0)})$ represents the nonradiative decay time of the S_j ($j = 1, 2$) state in the vicinity[19] of its electronic origin. Finally we assume that the major electronic relaxation pathways of the two lowest excited singlet states involves the nonradiative decay of $S_2^{(0)}$ to high vibronic components $S_1^{(V)}$ of the first excited singlet state, and the nonradiative decay of $S_1^{(0)}$ to the high vibronic components $S_0^{(V)}$ of the ground electronic states. In view of the ordinary Franck–Condon selection rules for radiative transitions we can assume that (in the absence of collisional deactivation of S_1 states) the $S_1^{(V)}$ levels will decay radiatively to highly vibrationally excited components $S_0^{(V)}$ [emitting in the same energy range as $S_1^{(0)} \rightarrow S_0^{(0)}$], and decay nonradiatively to superhighly excited vibrational components $S_0^{(V1)}$ of the ground electronic state (see Fig. 6). These $S_1^{(V)}$ levels can also be radiatively excited [with a cross section $\sigma(S_1 \rightarrow S_2)$] to superhigh vibrationally excited levels $S_2^{(V1)}$ of the second excited state, which can in turn emit to some very highly excited vibrational components of the ground state, or of the first excited state or decay nonradiatively. However, in view of the efficient internal conversion from S_1 we can terminate the cycle of events at this point. Finally we assert that under the lower power level employed herein (total output 10^{18} photons per pulse) the depletion of the ground electronic state $S_0^{(0)}$ is negligible. Denoting by $[S_0] = \sum_V [S_0^{(V)}]$, $[S_1] = \sum_V [S_1^{(V)}]$ and by $[S_2] = \sum_V [S_2^{(V)}]$, the total concentrations of the three lowest singlet states we have the simple kinetic equations

$$d[S_1]/dt = \sigma(S_0^0 \rightarrow S_1^0) I [S_0] - [\tau_r(S_1 \rightarrow S_0)^{-1} + \tau_{nr}(S_1)^{-1} + \sigma(S_1^0 \rightarrow S_2^0) I][S_1^-] + [\tau_r(S_2 \rightarrow S_1)^{-1} + \tau_{nr}(S_2)^{-1}][S_2], \quad (1)$$

$$d[S_2]/dt = \sigma(S_1^0 \rightarrow S_2^0) I [S_1] - [\tau_r(S_2 \rightarrow S_0)^{-1} + \tau_r(S_2 \rightarrow S_1)^{-1} + \tau_{nr}(S_2)^{-1}][S_2]. \quad (2)$$

Under steady state conditions, which are justified for the present experimental conditions the total blue fluorescence yield is

$$F_t^B = \frac{[S_2]}{\tau_r(S_2 \rightarrow S_0)} = \frac{\sigma(S_0^0 \rightarrow S_1^0)[S_0] Y(S_2 \rightarrow S_0) \sigma(S_1^0 \rightarrow S_2^0) I^2}{\tau_{nr}(S_1^0)^{-1} + \tau_r(S_1 \rightarrow S_0)^{-1} + \sigma(S_1^0 \rightarrow S_2^0) I [1 - \gamma(\tau_r(S_2 \rightarrow S_1)^{-1} - \tau_{nr}(S_2)^{-1})]}, \quad (3)$$

where

$$\gamma = \tau_r(S_2 \rightarrow S_0) Y(S_2 \rightarrow S_0).$$

As $\tau_r(S_2 \rightarrow S_1) \gg \tau_{nr}(S_i)$, we have

$$F_t^B = \frac{\sigma(S_0^0 \rightarrow S_1^0)[S_0] \sigma(S_1^0 \rightarrow S_2^0) Y(S_2 \rightarrow S_0) I^2}{\tau_{nr}(S_1^0)^{-1} + \sigma(S_1^0 \rightarrow S_2^0) Y(S_2 \rightarrow S_0) I}. \quad (4)$$

The square dependence of F_t^B in I^2 (Fig. 2) implies that in the laser intensity region employed by us the contribution of the second term in the denominator of (4) is negligible, the value which we shall derive for $\sigma(S_1^0 \rightarrow S_2^0)$ is consistent with this assertion. Thus, under our experimental conditions, we have

$$F_t^B = \sigma(S_0^0 \rightarrow S_1^0)[S_0] \sigma(S_1^0 \rightarrow S_2^0) \tau_{nr}(S_1^0) Y(S_2 \rightarrow S_0) I^2. \quad (5)$$

Utilizing our experimental values $K = 5 \times 10^{-33}$ photon^{-1}·cm·sec^{-1} and $\sigma(S_0^0 \rightarrow S_1^0)[S_0] = 0.22$, the value of $\tau_{nr}(S_1^0)$ just obtained and the (estimated) value of $Y(S_2^0 \rightarrow S_1^0) = 0.2$ we get $\sigma(S_1^0 \rightarrow S_2^0) = 1 \times 10^{-20}$ cm^2 at 6943 Å. A cross check on this estimate is obtained from the blue to red emission ratio $R_1 = 4.5 \times 10^{-2}$ (see Sec. III.B) at $I = 1.8 \times 10^{24}$ photons·cm^{-2}·sec^{-1}, which is given by $R_1 = \sigma(S_1^0 \rightarrow S_2^0) I \tau_r(S_1 \rightarrow S_0)/\tau_r(S_2 \rightarrow S_0)$ taking $\gamma = 10^{-9}$ sec we obtain $\sigma(S_0^0 \rightarrow S_2^0) = 2 \times 10^{-21}$ cm^2, which agrees within the claimed accuracy with our previous result. This low cross section for the $S_1^0 \rightarrow S_2^0$ absorption is consistent with the long lifetime $\tau_r \times (S_2 \rightarrow S_1) = 2 \times 10^{-6}$ sec for the spin allowed radiative decay between the two excited singlet states. These results for the absorption cross sections and radiative decay time clearly demonstrate that although the $S_1 \rightarrow S_2$, $^1B_1(1) \rightarrow {}^1A_1(2)$ transition is symmetry allowed its oscillator strength is rather low. This conclusion is consistent with the theoretical calculations[27] of Pariser which demonstrated that the oscillator strength for the

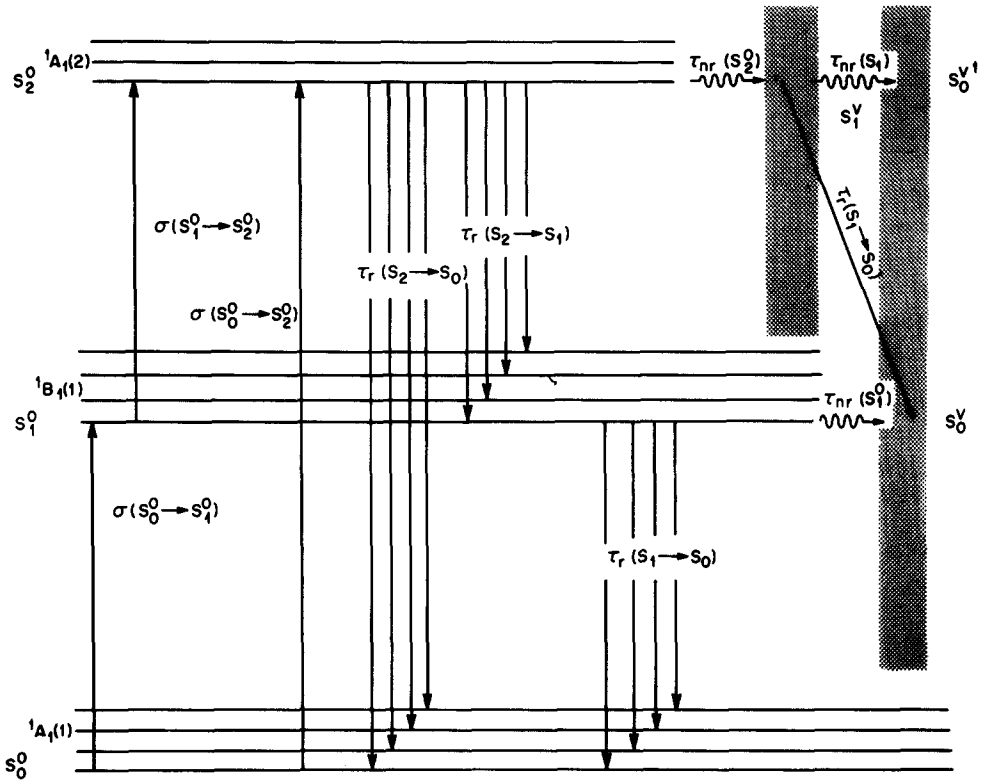

FIG. 6. Energy levels diagram for azulene.

triplet $^3B_1(1) \rightarrow {}^3A_1(2)$ transition of azulene at fixed nuclear configuration is lower than 10^{-3}. An additional contribution to the oscillator strength of the $S_1 \rightarrow S_2$ transition may arise, of course, from the Herzberg–Teller vibronic coupling mechanism. The experimentally estimated pure radiative decay time $\tau_r(S_2 \rightarrow S_1) \approx 2 \times 10^{-6}$ sec is of the same order of magnitude as for spin allowed vibronically induced transitions in benzene[22] and $n \rightarrow \pi^*$ excitation in ketones.[28]

IV. DISCUSSION

In this paper we report the results of an experimental study of the decay of the two lowest excited singlet states of the azulene molecule in the gas phase. Because of inherent experimental difficulties these data had to be recorded at moderately high azulene pressure ($\sim 5 \times 10^{-3} M$) and in the presence of $1.5 \times 10^{-2} M$ He gas (250 torr at 30°C). The "isolated" molecule case can be

TABLE I. Decay characteristics of the two lowest excited singlet states of azulene.

			Gas phase data (present work)				Solution data	
i	j	Transition $S_i \rightarrow S_j$	$Y(S_i^0 \rightarrow S_0)$	$\tau_{nr}(S_i^0)$ [sec]	$\sigma(S_j \rightarrow S_i)$ cm^2	$\tau_r(S_i \rightarrow S_j)$ [sec]	$Y(S_i \rightarrow S_0)$	$\tau_{nr}(S_i)$ [sec]
1	0	$S_1 \rightarrow S_0$	8×10^{-6}	7×10^{-12}	1×10^{-19} [a] 5×10^{-19} [d]	8×10^{-7} [b]	10^{-6} [c]	7.5×10^{-12} [c] 6×10^{-12} [e]
2	1	$S_2 \rightarrow S_1$	5×10^{-4}	1×10^{-9} [f]	1×10^{-20} [g]	2×10^{-6}	10^{-7} [h]	1.2×10^{-9} [i]
2	0	$S_2 \rightarrow S_0$	0.2 ± 0.1 [f]	1×10^{-9} [f]	1.2×10^{-18} [a] 6×10^{-18} [d]	5×10^{-9} [b]	0.24[i]	1.2×10^{-9} [i]

[a] Estimated from solution spectra near the origin of the electronic states.
[b] Solution data for the integrated oscillator strength.
[c] References 11 and 12. Decay from S_1 ($v = 5$) in solution.
[d] Reference 16.
[e] E. Drendt, G. M. Van der Deijl, and P. J. Zandstra, Chem. Phys. Letters **2**, 526 (1968). Decay from S_1 ($V = 0$).
[f] Based on a semiquantitative comparison of the emission quantum yields of azulene in the gas phase and in solution.
[g] Experimental result near the band origin (present work).
[h] Estimated near the band maxima.
[i] Reference 16.

realized provided that the time τ_c between collision with the electronically excited azulene molecule is long compared to the lifetime for the decay of the excited state. For a reasonable collision diameter of 5 Å the gas kinetic collision probability is $z=7\times10^6$ sec$^{-1}\cdot$torr^{-1}. Thus the time between collisions of the electronically excited azulene molecule with He is $\tau_c=5\times10^{-10}$ sec. Thus $\tau_c\gg\tau_{nr}(S_1^0)$ and we can consider the decay of the S_1 state as originating from the isolated molecule. On the other hand, during the decay of the S_2 state which is characterized by a total decay time of $(1-2)\times10^{-9}$ sec the excited molecule collides with the buffer gas.

In Table I we have assembled the pertinent data concerning the direct information concerning the emission quantum yields, and the absorption cross section and the indirect information concerning the nonradiative decay for the S_0, S_1, and S_2 states of the azulene in the gas phase, obtained herein by excitation by a Q switched ruby laser and its second harmonic. These results are compared with the available solution data previously measured by picosecond spectroscopy.[11–16] Referring to the general motivations of the present study as outlined in the introduction we would like to point out that:

(a) The nonradiative decay of S_1^0 for the (practically) "isolated" azulene molecule in the gas phase practically coincides (within an uncertainty of a numerical factor of 2) with the solution data,[11,12] thus we provide an experimental confirmation of the theoretical predictions[1] for intramolecular electronic relaxations in the statistical limit, which should be the same for the "isolated" molecule and for the molecule imbedded in an inert medium. It should be also pointed out that the decay characteristics of the S_2 state (near its electronic origin), which is however perturbed by the He gas, were also found to be similar in the gas phase and in solution.

(b) The information obtained herein concerning the decay characteristics of the first excited singlet state of the azulene molecule utilizing a moderately low power (100 MW) "long time" (10–20 nsec) excitation by a Q switched laser, coincides with the direct results obtained by ultra short picosecond excitation utilizing high power (10 GW) pulses.

(c) The emission quantum yield for the $S_2\rightarrow S_1$ transition observed by us utilizing a second harmonic Q switched pulse from a ruby laser is higher by about 2–3 orders of magnitude than the previous result obtained by utilizing the second harmonic of the mode locked ruby laser. A possible explanation of the discrepancy between these results is that under high power excitation $S_2\rightarrow S_0$ stimulated emission may occur, which is characterized by a high quantum yield, and which will increase the branching ratio between the $S_2\rightarrow S_0$ and $S_2\rightarrow S_1$ emission. This point deserves a further study. Note that in view of the low $S_2\rightarrow S_1$ emission quantum yield stimulated emission between excited states is not expected to occur. Finally it is worthwhile noticing that $S_1\rightarrow S_0$ stimulated emission will be not exhibited under ultrashort pulse, high power, excitation conditions in view of the efficient nonradiative decay of S_1.

ACKNOWLEDGMENTS

We are grateful to M. Levine and to R. David for the valuable assistance. This research was partially supported by a grant from the Israel Broida Memorial Fund of the P.E.F. Israel Endowment Fund.

[1] J. Jortner, J. Chim. Phys. **67,** 7 (1970).
[2] M. Beer and H. C. Longuett-Higgins, J. Chem. Phys. **23,** 1390 (1955).
[3] J. W. Siedman and D. S. McClure, J. Chem. Phys. **24,** 757 (1956).
[4] G. Vismawath and M. Kaska, J. Chem. Phys. **24,** 574 (1956).
[5] Z. S. Ruzevich, Opt. Spektrosk. **15,** 357 (1963) [Opt. Spectrosc. **15,** 191 (1963)].
[6] G. Binsch, E. Heibrooner, R. Jankow, and D. Schmidt, Chem. Phys. Letters **1,** 135 (1967).
[7] R. C. Dhingra and J. A. Poole, Chem. Phys. Letters **2,** 108 (1968).
[8] R. C. Dhingra and J. A. Poole, J. Chem. Phys. **48,** 4829 (1968).
[9] P. M. Rentzepis and M. A. Duguay, Appl. Phys. Letters **8,** 118 (1967).
[10] P. M. Rentzepis, C. J. Mitschelle, and A. C. Saxman, Appl. Phys. Letters **17,** 122 (1970).
[11] P. M. Rentzepis, Science **169,** 239 (1970).
[12] (a) P. M. Rentzepis, Chem. Phys. Letters **2,** 117 (1968). (b) P. M. Rentzepis, Chem. Phys. Letters **3,** 717 (1969).
[13] The major pathway for the radiationless decay of S_1 involves S_1-S_0 internal conversion (Refs. 11, 12) rather than S_1-T_1 intersystem crossing.
[14] P. M. Rentzepis, Photochem. Photobiol. **2,** 578 (1968).
[15] P. W. Wannier, P. M. Rentzepis, and J. Jortner, Chem. Phys. Letters **10,** 102 (1971); **10,** 193 (1971).
[16] P. M. Rentzepis, J. Jortner, and R. P. Jones, Chem. Phys. Letters **4,** 599 (1970).
[17] M. Kasha, Discussions Faraday Soc. **9,** 14 (1950).
[18] R. E. Kellog, J. Chem. Phys. **44,** 411 (1966).
[19] W. R. Ware and P. T. Cunningham, J. Chem. Phys. **44,** 4763 (1966).
[20] L. G. Anderson and C. S. Parameter, J. Chem. Phys. **52,** 466 (1970).
[21] E. Drent and J. Kommandeur (unpublished); see also A. Nitzan, J. Jortner, E. Drent, and J. Kommandeur, Chem. Phys. Letters (to be published).
[22] J. B. Birks, *Photophysics of Aromatic Molecules* (Wiley, New York, 1970).
[23] D. Huppert, J. Jortner, and P. M. Rentzepis, Chem. Phys. Letters **13,** 225 (1972).
[24] I. B. Berlman *Handbook of Fluorescence Spectra of Aromatic Molecules* (Academic, N.Y., 1965).
[25] J. P. Byrne and I. G. Ross, Australian J. Chem. **24,** 1107 (1971).
[26] W. Siebrand and D. F. Williams, J. Chem. Phys. **44,** 1860 (1969).
[27] R. Pariser, J. Chem. Phys. **25,** 1112 (1956).
[28] G. E. Busch, P. M. Rentzepis, and J. Jortner, J. Chem. Phys. **56,** 361 (1972).